Identification of a transcriptional signature found in multiple models of ASD and related disorders

Samuel Thudium,[1,2] Katherine Palozola,[1,2] Éloïse L'Her,[1,2] and Erica Korb[1,2]

[1]Department of Genetics, Perelman School of Medicine at the University of Pennsylvania, Philadelphia, Pennsylvania 19104, USA; [2]Epigenetics Institute, Perelman School of Medicine at the University of Pennsylvania, Philadelphia, Pennsylvania 19104, USA

Epigenetic regulation plays a critical role in many neurodevelopmental disorders (NDDs), including autism spectrum disorder (ASD). In particular, many such disorders are the result of mutations in genes that encode chromatin-modifying proteins. However, although these disorders share many features, it is unclear whether they also share gene expression disruptions resulting from the aberrant regulation of chromatin. We examined five chromatin modifiers that are all linked to ASD despite their different roles in regulating chromatin. Specifically, we depleted ASH1L, CHD8, CREBBP, EHMT1, and NSD1 in parallel in a highly controlled neuronal culture system. We then identified sets of shared genes, or transcriptional signatures, that are differentially expressed following loss of multiple ASD-linked chromatin modifiers. We examined the functions of genes within the transcriptional signatures and found an enrichment in many neurotransmitter transport genes and activity-dependent genes. In addition, these genes are enriched for specific chromatin features such as bivalent domains that allow for highly dynamic regulation of gene expression. The down-regulated transcriptional signature is also observed within multiple mouse models of NDDs that result in ASD, but not those only associated with intellectual disability. Finally, the down-regulated transcriptional signature can distinguish between control and idiopathic ASD patient iPSC-derived neurons as well as postmortem tissue, demonstrating that this gene set is relevant to the human disorder. This work identifies a transcriptional signature that is found within many neurodevelopmental syndromes, helping to elucidate the link between epigenetic regulation and the underlying cellular mechanisms that result in ASD.

[Supplemental material is available for this article.]

Neurodevelopmental disorders (NDDs) that result in autism spectrum disorder (ASD) are caused by both environmental and genetic factors. Even within the subset of disorders that have a clear genetic cause, each individual syndrome stems from a unique mutation in an increasingly long list of ASD susceptibility genes. Such heterogeneity has made it difficult to develop a unifying model of the disruptions that lead to shared phenotypes or to develop treatments that address shared underlying causes. However, recent studies demonstrated that a disproportionate number of ASD susceptibility genes encode epigenetic regulators (O'Roak et al. 2012; Parikshak et al. 2013; De Rubeis et al. 2014; Iossifov et al. 2014). In particular, many such mutations are found in proteins that regulate chromatin, the complex of DNA and histone proteins that helps to regulate transcription.

Histones are regulated by numerous post-translational modifications, such as acetylation and methylation, that ultimately affect transcription. These modifications recruit transcriptional regulators and allow chromatin to transition between open and closed states that are permissive or repressive to transcription, thus providing a complex code that regulates gene expression (Strahl and Allis 2000; Turner 2000; Jenuwein and Allis 2001; Berger 2007). The importance of this "histone code" is becoming increasingly appreciated in neuroscience, from its function in memory formation to its involvement in NDDs (Borrelli et al. 2008; Peixoto and Abel 2013; Rangasamy et al. 2013). However, it remains unclear if different forms of syndromic ASD that result from mutations in distinct chromatin regulators share transcriptional disruptions.

Determining whether disruption of multiple syndromic ASD-linked chromatin modifiers with disparate functions leads to overlapping gene expression changes presents multiple challenges. Thus far, such chromatin modifiers have been analyzed individually in different systems but never in parallel in a controlled genetic background. As a result, although our understanding of these disorders has improved drastically in recent years, previous studies were not designed to allow for a comparison between different causes of ASD or to identify common pathways that underlie shared phenotypes. Work examining the effects of loss of these chromatin-modifying proteins in animals is also confounded by the full body and lifelong loss of these proteins throughout development. Thus, the complexity of the compensatory response and other related health effects may occlude any relevant transcriptional signature that could answer these outstanding questions. Finally, many NDDs result in a range of phenotypes and often cause both ASD and intellectual disability (ID), so identifying which underlying epigenetic disruptions are associated with one or both phenotypes pose additional hurdles. To overcome these challenges, we examined the effects of depleting multiple ASD-linked chromatin modifiers in parallel, in neurons in a controlled genetic background, with the goal of defining the common gene expression patterns shared across multiple forms of ASD. Identifying such patterns has the potential to provide novel insights into the cellular disruptions that contribute to ASD and

1642 **Genome Research**
www.genome.org
32:1642–1654 Published by Cold Spring Harbor Laboratory Press; ISSN 1088-9051/22; www.genome.org

how mutations in a diverse array of histone-modifying enzymes can lead to common phenotypic outputs.

Results

Defining gene expression profiles of syndromic ASD-linked chromatin modifiers

We sought to determine if the loss of different chromatin-modifying enzymes linked to related NDDs results in a common transcriptional signature. To define such a signature, we focused on five chromatin modifiers, ASH1L, CHD8, CREBBP, EHMT1, and NSD1, associated with syndromes that include ID and ASD traits (Table 1). Of the many chromatin regulators linked to such disorders (Neale et al. 2012; O'Roak et al. 2012; Sanders et al. 2012; De Rubeis et al. 2014; Iossifov et al. 2014), we chose from the subset that led to well-defined syndromes caused by loss-of-function mutations or deletions (Petrif et al. 1995; Tanaka et al. 1997; Bartsch et al. 1999; Kurotaki et al. 2002; Douglas et al. 2003; Kleefstra et al. 2006; Schorry et al. 2008; Abrahams et al. 2013; Okamoto et al. 2017; Stessman et al. 2017). This ensured that we examined proteins whose loss results in NDDs with high penetrance. We further selected for chromatin regulators with mouse models that recapitulate the features of the associated disorder to ensure that mouse neuronal models are an appropriate system in which to study their function (Coupry et al. 2002; Kurotaki et al. 2002; Niikawa 2004; Kleefstra et al. 2006, 2009; Neale et al. 2012; Bernier et al. 2014; Eram et al. 2015; Benevento et al. 2016; Shen et al. 2019; Gao et al. 2021). In addition, these five proteins are among the top ASD risk genes as identified by TADA analysis (Fu et al. 2021), with four of the five in the top 100 susceptibility genes for idiopathic ASD. They also fall into the same gene expression module (based on BrainSpan data), which contains the greatest enrichment of ASD susceptibility genes (Miller et al. 2014; Ji et al. 2016). Finally, we selected a set of chromatin modifiers that have a diverse array of functions in chromatin. These proteins target different substrates in chromatin, including modifying different histone proteins and residues. They also perform a diverse array of functions such as adding different types of modifications. For example, CREBBP acetylates histones; EHMT1 methylates H3K9; and ASH1L and NSD1 promote different methylation states of H3K36 (Tachibana et al. 2008; Thompson et al. 2008; Jin et al. 2011; Qiao et al. 2011; Miyazaki et al. 2013). Further, some are associated with active gene expression (CREBBP, ASH1L, NSD1) whereas others are associated with repressive gene expression

(EHMT1, CHD8). Thus, we would not expect these proteins to target the same set of genes or their loss to result in similar transcriptional profiles solely based on having shared functions in modulating chromatin. Instead, the major commonality between these proteins is that their disruption leads to ID and ASD, so any overlapping gene expression changes are more likely to be relevant to shared phenotypic output.

To study the effects of the loss of these chromatin modifiers in parallel, we used a primary neuronal culture system and lentiviral shRNA knockdown of each chromatin modifier (Fig. 1A). There are several advantages to this approach: (1) This culture method generates a purely neuronal population (Brockes et al. 1979; Dotti et al. 1988; Korb et al. 2015) and thus avoids the heterogeneity of brain tissue and the compounding effects of a system-wide knockout (KO); (2) neurons are cultured from embryonic mouse brains (E16.5), which allows for the investigation of early neuronal development time points that are relevant to the onset of NDDs and ASD; (3) neurons are analyzed 5 d after knockdown, thus avoiding long-term compensatory responses resulting from lifelong loss of function; (4) within each biological replicate derived from separate litters, each candidate gene is knocked down simultaneously from neurons cultured from the same embryos (with both male and female pups pooled), thereby controlling for both genetic background (C57BL/6J), developmental time point, and variation between animals; and (5) multiple replicates can be generated and processed in parallel to allow for a high degree of rigor using true biological replicates (each coming from separate litters of mice) while also minimizing technical variability. Although ID and ASD can be caused by atypical brain region connectivity that cannot be detected in our system, our goal is to define the underlying cellular mechanisms within neurons that ultimately lead to wider disruptions.

Primary cultured neurons were infected with lentiviruses containing shRNAs targeting each syndromic ASD-linked chromatin modifier or with a nontargeting control shRNA at 5 d in culture. Neurons were then collected 5 d after infection to allow for robust depletion of target proteins. We used RT-qPCR to examine the degree of knockdown achieved through lentiviral infection and confirmed depletion of all target transcripts (Supplemental Fig. 1A–E). In most cases, both RT-qPCR and RNA sequencing (RNA-seq) data (Fig. 1B–F; Supplemental Fig. 1A–J) demonstrated that depletion of each chromatin modifier specifically caused loss of only that target without disrupting expression of the other four targets. This suggests that these five chromatin modifiers do not directly target each other. We further confirmed knockdown of the target

Table 1. Candidate proteins

Protein	Function	Target (mark)	Associated syndrome	ASD	ID	Ms
ASH1L	Histone lysine methyltransferase	H3K36 (me3)	Emerging MCA/ID disorder	X	X	X
CHD8	Chromodomain helicase	Chromatin remodeler; recruitment of other complexes	Autism 18; CHARGE syndrome	X	X	X
CREBBP	Histone acetyltransferase	Promiscuous; H3 lysines (Ac)	Rubinstein–Taybi syndrome	X	X	X
EHMT1	Histone lysine methyltransferase	H3K9 (me1/me2)	Kleefstra syndrome	X	X	X
NSD1	Histone lysine methyltransferase	H3K36 (me2)	Sotos syndrome; Beckwith–Wiedemann syndrome	X	X	X

Functions and associated disorders of five chromatin modifiers chosen for analysis. All proteins have distinct functions in regulating histones. Mutation or deletion of all candidates results in well-defined neurodevelopmental syndromes that include features such as intellectual disability (ID) and autism spectrum disorder (ASD). Mouse (Ms) column indicates a mouse model shows expected phenotypes.
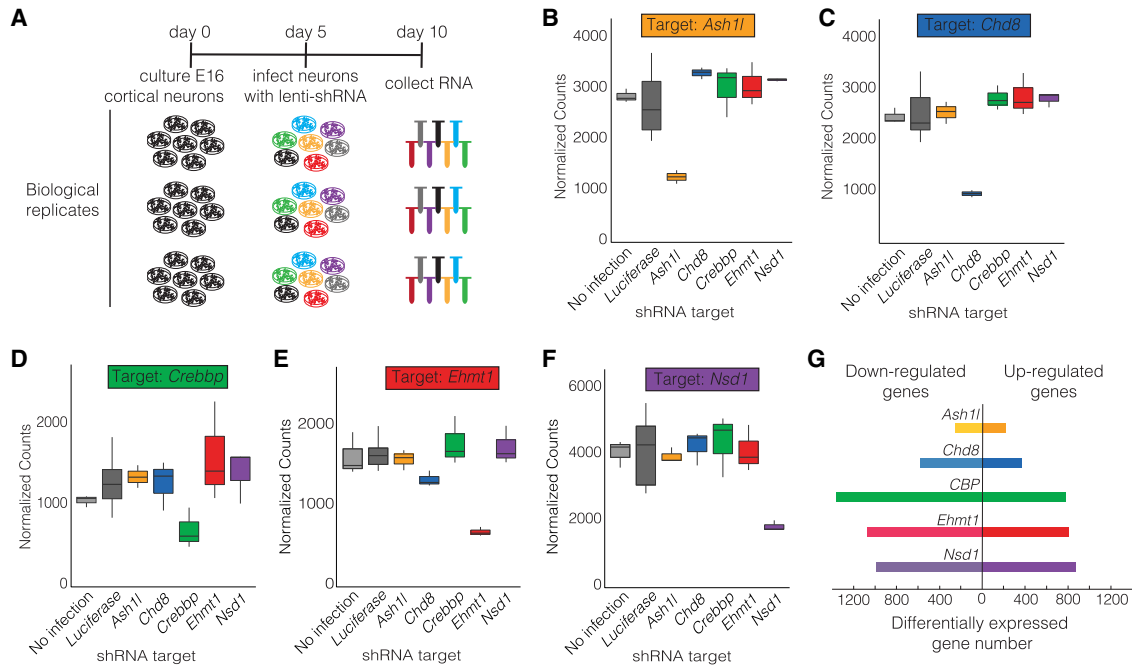
Figure 1. System for comparison of gene expression profiles of chromatin modifiers. (*A*) Primary neuronal culture system used to analyze gene expression changes after knockdown of ASD-linked chromatin modifiers. (*B–F*) Expression of chromatin modifiers following knockdown, from RNA sequencing data. (*G*) Number of genes down- and up-regulated by knockdown of five ASD-linked chromatin-associated genes. N = 3 replicates.

proteins in all cases in which antibodies were available (Supplemental Fig. 1K–O). In addition, knockdown of these targets did not change the identity of cultured neurons (Supplemental Fig. 1P,Q).
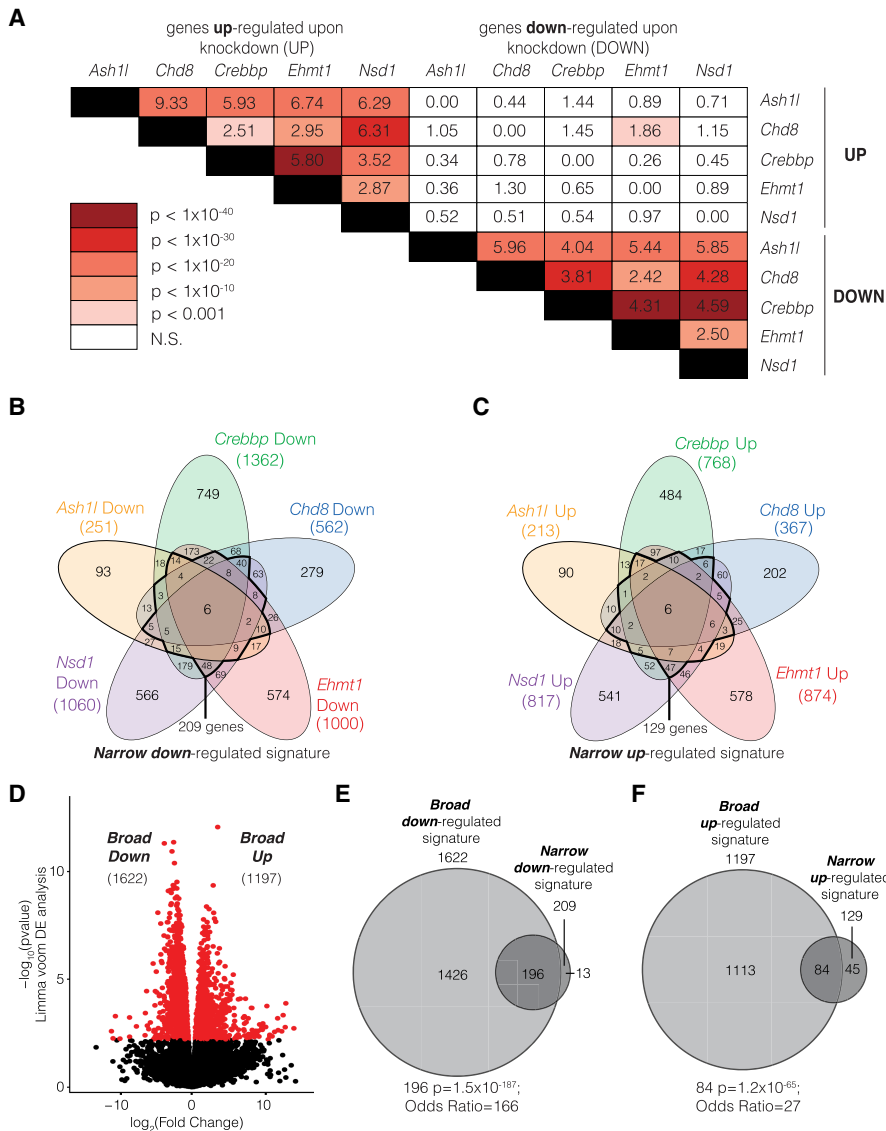
Having confirmed knockdown of all targets, we used RNA-seq results to define gene expression changes resulting from knockdown of all five chromatin-associated proteins. As expected, in all cases knockdown resulted in robust gene expression changes, with genes both increased and decreased in expression compared with nontargeting control shRNA infection (Fig. 1G; Supplemental Fig. 2A–E; Supplemental Table 1).

Overlap of gene expression changes caused by loss of ASD-linked chromatin modifiers

To examine potential overlap in the resulting gene expression changes, we took several approaches. First, we examined the direct overlap of each possible pairwise comparison and used a hypergeometric test to determine the significance of the number of overlapping genes. We found that direct comparison of every down-regulated gene set was significant, and the same was true of each up-regulated gene set overlap (Fig. 2A). Conversely, comparison of each up-regulated gene set with each down-regulated gene set yielded almost no significant overlaps. These findings indicate that many of the same genes are differentially regulated by these five ASD-linked chromatin modifiers. Given that these five chromatin modifiers were chosen specifically based on their divergent functions in regulating chromatin, their depletion would not necessarily be expected to have similar direct effects on gene expression. Instead, the significance of these overlaps indicates that this subset of genes may be particularly sensitive to disruption of ASD-linked chromatin modifiers in neurons.

We next sought to ensure that these overlapping gene sets did not arise due to unintended changes occurring in neurons in response to the nontargeting shRNA control lentivirus such that knockdown of any other target would appear to produce a similar disruption. Notably, very few genes were differentially expressed when comparing the no infection condition to the nontargeting control viral infection, suggesting that this virus did not cause widespread changes in gene expression (Supplemental Fig. 2F). To further rule out any possible confounding factor resulting from the use of a nontargeting shRNA virus as a control condition, we repeated all differential gene expression analysis using the non-infected control condition as our baseline (Supplemental Fig. 3A, B). We found that similar gene sets were identified regardless of the control condition used, producing highly significant overlaps in each case. Further, in all cases, fewer differentially expressed genes were identified when the nontargeting shRNA lentivirus was used as a control, indicating that this is a slightly more stringent control and likely accounts for any modest gene expression changes resulting from the cellular response to infection. We therefore proceeded with this as the main control condition for subsequent analysis.

We next examined all higher-order intersections between these gene sets to determine which genes are commonly disrupted in response to knockdown of multiple ID/ASD-linked chromatin modifiers (Fig. 2B,C). Only six genes were common between all data sets for both up-regulated (*Trak2*, *Snap29*, *Prickle1*, *Ccnt1*, *Ppig*, and *Fam214b*) and down-regulated (*Fcgrt*, *Dbp*, *Myorg*, *Creb3l1*, *Ret*, and *Isoc1*) genes. However, 209 down-regulated and 133 up-regulated genes were shared by knockdown of the majority (at least three of the five) of the ASD-linked chromatin modifiers. Notably, four of the 133 up-regulated genes were also found in the comparison between noninfected neurons and neurons infected with nontargeting shRNA virus and were excluded from

A

Figure 2A heatmap. Columns: genes **up**-regulated upon knockdown (UP) — Ash1l, Chd8, Crebbp, Ehmt1, Nsd1; genes **down**-regulated upon knockdown (DOWN) — Ash1l, Chd8, Crebbp, Ehmt1, Nsd1.

	UP: Ash1l	UP: Chd8	UP: Crebbp	UP: Ehmt1	UP: Nsd1	DOWN: Ash1l	DOWN: Chd8	DOWN: Crebbp	DOWN: Ehmt1	DOWN: Nsd1	
Ash1l		9.33	5.93	6.74	6.29	0.00	0.44	1.44	0.89	0.71	UP
Chd8			2.51	2.95	6.31	1.05	0.00	1.45	1.86	1.15	
Crebbp				5.80	3.52	0.34	0.78	0.00	0.26	0.45	
Ehmt1					2.87	0.36	1.30	0.65	0.00	0.89	
Nsd1						0.52	0.51	0.54	0.97	0.00	
Ash1l							5.96	4.04	5.44	5.85	DOWN
Chd8								3.81	2.42	4.28	
Crebbp									4.31	4.59	
Ehmt1										2.50	
Nsd1											

Legend:
- $p < 1 \times 10^{-40}$
- $p < 1 \times 10^{-30}$
- $p < 1 \times 10^{-20}$
- $p < 1 \times 10^{-10}$
- $p < 0.001$
- N.S.

B

Crebbp Down (1362); Ash1l Down (251); Chd8 Down (562); Nsd1 Down (1060); Ehmt1 Down (1000). 749, 93, 279, 566, 574, 6, 209 genes. **Narrow down**-regulated signature

C

Crebbp Up (768); Ash1l Up (213); Chd8 Up (367); Nsd1 Up (817); Ehmt1 Up (874). 484, 90, 202, 541, 578, 6, 129 genes. **Narrow up**-regulated signature

D

Broad Down (1622); Broad Up (1197). x-axis: $\log_2(\text{Fold Change})$; y-axis: $-\log_{10}(\text{pvalue})$ Limma voom DE analysis

E

Broad down-regulated signature 1622; **Narrow down**-regulated signature 209. 1426, 196, 13. 196 $p = 1.5 \times 10^{-187}$; Odds Ratio = 166

F

Broad up-regulated signature 1197; **Narrow up**-regulated signature 129. 1113, 84, 45. 84 $p = 1.2 \times 10^{-65}$; Odds Ratio = 27

Figure 2. Overlap of genes that are differentially expressed following knockdown of ASD-linked chromatin modifiers. (*A*) Significance of overlap of down- and up-regulated genes after knockdown. Heatmap indicates significance level by hypergeometric testing. Numbers indicate odds ratio. (*B,C*) Overlap of genes that are down-regulated (*B*) or up-regulated (*C*) by multiple targets. Dark line indicates subset of genes differentially expressed in at least three of five gene sets used to define a "narrow" transcriptional signature. (*D*) Identification of commonly disrupted genes using *limma* voom differential expression analysis to generate a "broad" transcriptional signature. (*E,F*) Overlap of broad and narrow down (*E*) and up (*F*) signatures. Overlap significance; hypergeometric tests.

these gene sets to those identified by directly overlapping individual differentially expressed gene sets. We found that for both up- and down-regulated genes, *limma* analysis gene sets encompassed the majority of the genes found through overlap (Fig. 2E,F), indicating that this approach identified the same subset of commonly disrupted genes as well as additional genes.
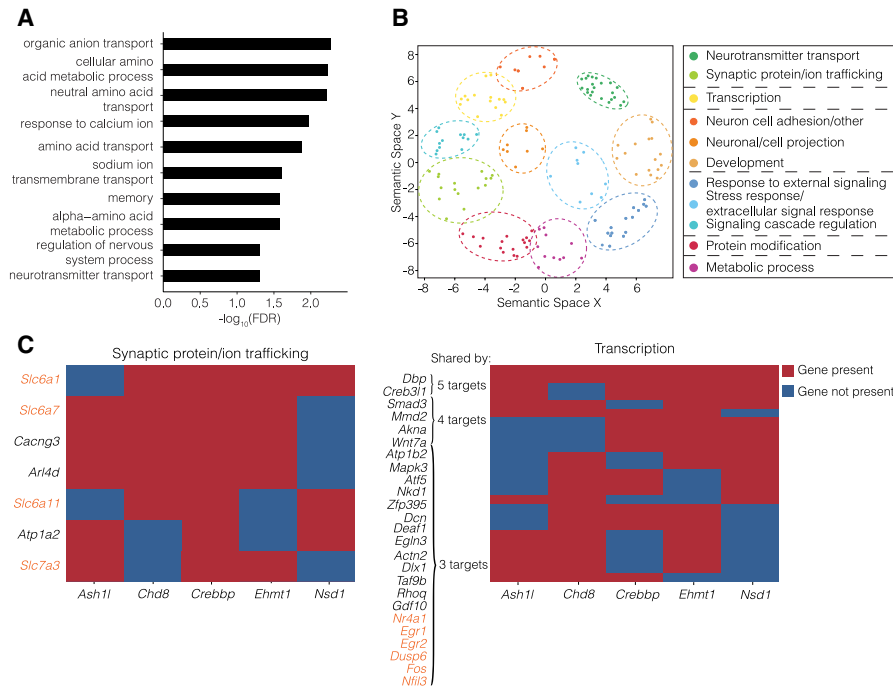
For simplicity, we will refer to the sets of genes that are up- or down-regulated in response to the majority of these chromatin modifiers as measured by direct overlap of single DEG lists as *narrow transcriptional signatures*. Those genes identified by *limma* analysis of the merged data set will be identified as *broad transcriptional signatures* (Supplemental Table 2). Given the greater number of down-regulated genes shared between the five chromatin modifiers in both statistical approaches, here we will largely focus on the down-regulated gene signature and include all analyses of the up-regulated signature in the Supplemental Figures.

Functional enrichments in the transcriptional signatures

We first sought to define the gene functions encoded by the up and down transcriptional signatures using Gene Ontology (GO) analysis (Mi et al. 2021). We found that the top enriched terms for the broad down-regulated signature included processes such as those related to ion trafficking and neurotransmitter transport (Fig. 3A; Supplemental Table 3). Although the narrow transcriptional down-regulated signature did not yield significant GO terms through traditional GO analysis, we also performed GeneWalk (Ietswaart et al. 2021), which uses network representation learning on a combined gene-regulatory and GO-term network constructed from input genes to elucidate significant gene functions that are relevant to the biological context of a given experiment (Supplemental Table 4). We then used REVIGO (Supek et al. 2011) to remove redundant outputs and cluster related functions, and labeled each resulting cluster with a descriptive identifier that encompassed the GO terms included (Fig. 3B; Supplemental Table 7). The GeneWalk output matched the standard GO analysis, demonstrating that these functional groups are enriched in the down-regulated transcriptional signature regardless of the methods used.

We next sought to define the specific genes within the transcriptional signature responsible for driving these functional enrichments. We identified the genes driving the enrichment of the top GeneWalk GO terms and determined how many of the five gene sets contained these gene drivers (Fig. 3C;

subsequent analyses. Thus, although these ASD-linked chromatin modifiers all have different functions in regulating chromatin and target different histone residues and genomic regions, the gene expression changes resulting from their depletion converge on common subsets of genes, particularly for down-regulated genes.

Given these unexpected highly significant overlaps, we sought to define commonly disrupted gene sets using an alternative statistical approach in addition to the direct overlap approach. We compared all knockdown conditions to nontargeting shRNA infected cells using *limma* voom differential expression analysis (Law et al. 2014; Ritchie et al. 2015). We identified a set of 1197 genes that were commonly up-regulated and 1622 genes that were commonly down-regulated (Fig. 2D). We then compared

Figure 3. Function of down-regulated transcriptional signature genes. (*A*) Gene Ontology (GO) analysis of down-regulated broad signature gene function. (*B*) GeneWalk analysis followed by REVIGO clustering of down-regulated narrow signature genes. (*C*) Genes contributing to main GO clusters that are differentially expressed after knockdown of three or more ASD-linked chromatin modifiers. Solute-carrier family and activity-dependent genes are shown in orange.

Supplemental Fig. 4A). Multiple members of the solute carrier family of genes, which regulate neurotransmitter transport, were present in at least three of the five gene sets contributing to the neurotransmitter and synaptic protein trafficking GO groups. We also found that many of the genes detected within at least three data sets for the "transcription" and "response to extracellular signal" GO groups identified through GeneWalk are well-established activity-dependent genes (also found in the corresponding standard GO terms "response to calcium ion" and "memory").

To directly examine whether activity-dependent genes were significantly enriched within the down-regulated transcriptional signatures, we used a previously generated set of genes up-regulated in neurons upon stimulation by brain-derived neurotrophic factor (BDNF) for 10 min (Korb et al. 2015). Upon comparing these lists, we found that both the narrow and broad down-regulated transcriptional signatures were significantly enriched for these genes, indicating that activity-dependent genes are among those preferentially disrupted by loss of ASD-linked chromatin modifiers (Supplemental Fig. 4B,C). We then confirmed these findings in an in vivo system by examining gene expression changes following a recall event in activated neurons using the TRAP2 mouse model (Supplemental Fig. 4D,E; Chen et al. 2020). Finally, we used RT-qPCR to confirm down-regulation of genes of interest following knockdown of the five ASD-associated chromatin modifiers, including several activity-dependent genes (*Fos* and *Nfil3*), a solute carrier family gene (*Slc7a3*), and a calcium channel gene (*Cacng1a*) (Supplemental Fig. 4F). We found that each of these genes was depleted in response to knockdown of at least four ASD-linked chromatin modifiers.

We performed similar analyses to identify functional groups enriched within the up-regulated transcriptional signatures.

Using standard GO, we found that the top 10 functional groups within broad signature genes largely included functions relevant to cell division (Supplemental Fig. 4G; Supplemental Table 3). Although neurons are postmitotic, they use many cell cycle genes for regulation of neuronal maturation and migration (Ohnuma and Harris 2003; Frank and Tsai 2009; Huang et al. 2010; Lim and Kaldis 2013). GeneWalk and REVIGO clustering of narrow up-regulated signature genes revealed enriched clusters including neuronal maturation that corresponded to the cell division gene sets found by GO (Supplemental Fig. 4H).

In addition to analyzing the transcriptional signatures defined above, we also examined the common functionally enriched groups shared between the ID/ASD-linked chromatin modifiers using a converse approach. We first performed GeneWalk on each of the five chromatin modifiers' up or down differentially expressed gene sets individually and then overlapped the resulting GO terms to define a set of ontology terms common to all gene sets (Supplemental Fig. 5A; Supplemental Tables 5–7). REVIGO was used to cluster output terms, and we identified each resulting cluster based on the GO terms included. We found functional groups for down-regulated genes through this approach that were equivalent to those found through GO and GeneWalk analysis of the ASD down-regulated signature, including responses to external signaling (containing activity-dependent genes) and synaptic protein trafficking (containing neurotransmitter transport genes) (Supplemental Fig. 5B). Similarly, by this alternate approach, we found many analogous functional clusters present in the GO terms shared by all up-regulated gene lists, such as cell morphology and development (Supplemental Fig. 5C). However, signature genes did not overlap with defined sets of ASD-risk genes (Supplemental Fig. 5D–G; Abrahams et al. 2013; Zhao et al. 2018). This suggests that loss of ASD-linked chromatin modifiers does not directly lead to depletion of other ASD-linked genes and instead targets a different subset of synaptic proteins, likely leading to synaptic dysfunction through independent mechanisms. Together, these data indicate that gene expression changes in response to loss of ID/ASD-linked chromatin modifiers affect critical neuronal regulatory processes such as neuronal development, synaptic trafficking, and activity-dependent gene regulation rather than by directly disrupting other known ASD-risk genes.

Chromatin features of the transcriptional signature

Having defined the functional relevance of the transcriptional signatures, we next sought to understand the features that make these genes particularly susceptible to disruption in response to knockdown of ASD-linked chromatin modifiers. We first examined their expression within control conditions and found, as expected, that they were all expressed within neurons but otherwise include a
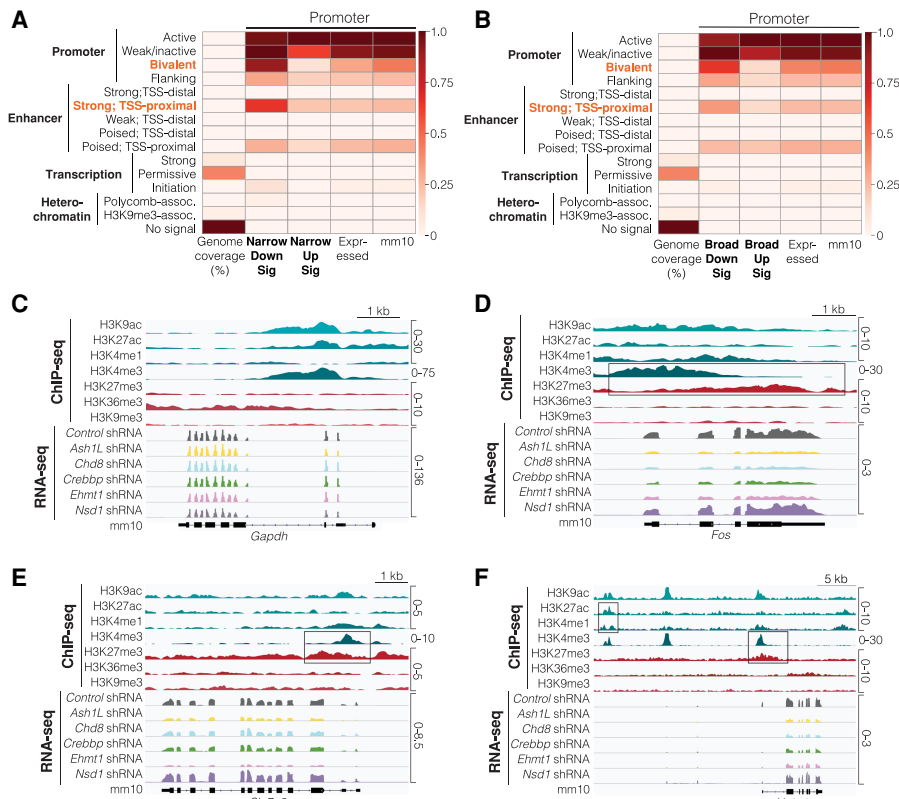
Figure 4. Chromatin states in transcriptional signature genes. (*A*) ChromHMM analysis of promoter (500 bp upstream of transcription start site [TSS]) of narrow transcriptional signature genes. (*B*) ChromHMM analysis of promoter (500 bp upstream of TSS) of broad transcriptional signature genes. (*C*) Gene track of a control gene, *Gapdh*, that is not regulated by ASD-linked chromatin modifiers. (*D–F*) Gene tracks of down-regulated transcriptional signature genes *Fos* (*D*), *Slc7a3* (*E*), and *Nr4a1* (*F*) that have bivalent domains (high H3K4me3 and high H3K27me3), low H3K36me3, and strong proximal enhancer sites (H3K4me1 and H3K27ac peaks upstream of *Nr4a1*) typical of down-regulated transcriptional signature genes. Boxes highlight these chromatin states. Expressed indicates genes expressed in neuronal culture system. Fold enrichments were calculated as the ratio of the fraction of bases in a given chromatin state that were present in our input gene coordinates of interest to the fraction of the genome described by the input gene coordinates. Displayed heatmaps represent overlap enrichment output values range-normalized by column.

which is associated with active gene promoters, and H3K27me3, which is associated with transcriptional repression. The synchronous presence of functionally opposing histone modifications allows for genes to be maintained in a poised state and rapidly activated in response to external signals (Bernstein et al. 2006; Voigt et al. 2013). In addition, the down-regulated transcriptional signatures were enriched for chromatin state corresponding to strong promoter-proximal enhancers, further indicating the presence of chromatin regulatory features that allow for the robust and highly regulated activation of target genes.

To ensure that the enrichment of these chromatin features is not dependent on the size of the region surrounding the TSS used to define the promoter and that the analysis did not inappropriately exclude features present in broader regions, we repeated ChromHMM with an expanded region upstream of the TSS and again found similar enrichment of these chromatin states (Supplemental Fig. 6E,F). We further sought to confirm that there is an enrichment of bivalent genes within these gene signatures. We found that a set of bivalent genes defined in E14.5 neocortical neurons (Albert et al. 2017) had a highly significant overlap with the down-regulated transcriptional signatures (Supplemental Fig. 6G–J), confirming an enrichment of bivalent chromatin states within the genes disrupted by depletion of ASD-linked chromatin modifiers.

Next, we plotted specific gene tracks of genes driving the functional GO enrichments, specifically activity-dependent genes and genes regulating neurotransmitter transport that were present in down-regulated transcriptional signatures. These genes contained bivalent domains with high H3K4me3 and H3K27me3 relative to ubiquitously expressed genes such as *Gapdh* (Fig. 4C–F). These genes also had low H3K36me3, which can repress aberrant transcription in actively transcribed genes. In genes containing proximal enhancers, such as *Nr4a1*, strong enhancer domains were marked by H3K4me1 and H3K27ac.

We also examined chromatin states of up-regulated transcriptional signature genes. Although down-regulated signature promoter coordinates were highly enriched for bivalent domains, we found that the opposite was true at the promoters of the up-regulated gene signatures; this was especially apparent in the more restrictive promoter region. Further, we saw robust enrichment of the active promoter state, marked by strong signals of H3K4me3, H3K9ac, and H3K27ac, in both the promoter regions of the up-regulated signature genes (Fig. 4A,B; Supplemental Fig. 6E,F). Together, these findings suggest that genes found within the transcriptional signatures may be particularly susceptible to disruption owing to distinct chromatin features. Down-regulated genes in particular have features of a poised chromatin state, such as
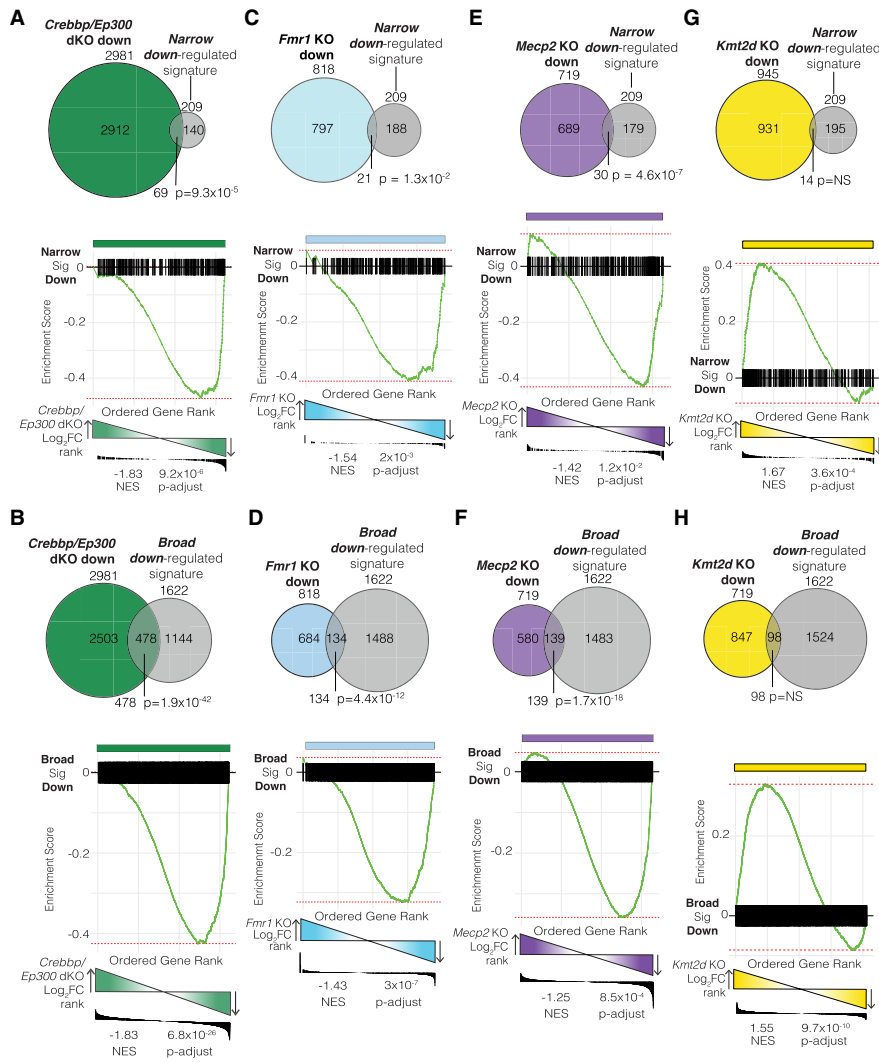
wide range of relative expression levels with no notable enrichment for low or high expressed genes (Supplemental Fig. 6A–D). Previous work has identified specific chromatin features that are shared between genes that are disrupted in NDDs (Zhao et al. 2018). We therefore examined the chromatin features found within these transcriptional signatures. We used ChromHMM (Ernst and Kellis 2017) on well-validated ChIP-seq data from E12.5 mouse forebrain tissue to identify the chromatin states enriched at the promoters of transcriptional signature genes (Fig. 4A,B; Supplemental Table 8). We compared transcriptional signature genes with the entire mouse genome, the genes expressed in neurons based on RNA-seq data, and all mm10 genes. As expected, the full genome was depleted of defined chromatin states relative to all gene sets examined. However, several features are distinct between the promoters of the down-regulated transcriptional signature genes compared with both the promoters of all genes and the promoters of the subset of genes expressed within neurons. In particular, promoters of the down-regulated transcriptional signature genes were enriched for a bivalent state. Bivalency refers to the co-occurrence of histone modifications associated with opposing functions and is typically defined by the presence of H3K4me3,

Figure 5. Identification of transcriptional signature in mouse models of ASD. (*A,B*) Overlap (*top*) and GSEA (*bottom*) analysis of the narrow (*A*) and broad (*B*) down-regulated transcriptional signature compared with differentially expressed genes in a *Crebbp/Ep300* (also known as *Kat3a/b*) double knockout (KO) mouse model. (*C,D*) Overlap and GSEA analysis of the narrow (*C*) and broad (*D*) down-regulated transcriptional signature compared with differentially expressed genes in an *Fmr1* KO mouse model of FXS. (*E,F*) Overlap and GSEA analysis of the narrow (*E*) and broad (*F*) down-regulated transcriptional signature compared with differentially expressed genes in a *Mecp2* KO mouse model of Rett syndrome. (*G, H*) Overlap and GSEA analysis of the narrow (*G*) and broad (*H*) down-regulated transcriptional signature compared with differentially expressed genes in a *Kmt2d* KO mouse model of Kabuki syndrome. Overlap significance based on hypergeometric tests. NES indicates normalized enrichment score.

gene expression changes occurring within the brain, we compared these signatures to gene expression changes in multiple mouse models of NDDs. We first examined a mouse model used to study the genes implicated in Rubenstein–Taybi syndrome, which is characterized by short stature, moderate to severe ID, features of ASD, and additional abnormalities such as heart and kidney defects. It is most often caused by mutations in *CREBBP* or *EP300* (also known as *KAT3A* and *KAT3B*, respectively), which have overlapping functions as histone acetyltransferases. CREBBP was one of five chromatin modifiers targeted in order to generate the transcriptional signatures here, and thus we would hypothesize that these signatures would be present in this model if they are relevant to an in vivo system. We used RNA-seq of hippocampal tissue from a mouse model containing a double KO of *Crebbp* and *Ep300* (Lipinski et al. 2020) and examined the direct overlap of differentially expressed genes to the transcriptional signatures. We found a highly significant overlap between genes down-regulated in this KO model and both the narrow and broad down-regulated transcriptional signatures. As an alternate approach, we used gene set enrichment analysis (GSEA) to map down-regulated transcriptional signature genes onto a $\log_2$ fold change ranked list of all gene expression changes in *Crebbp/Ep300* double KO mice. Again, we found a highly significant enrichment through this analysis with down-regulated transcriptional signature genes present within highly down-regulated genes in the *Crebbp/Ep300* double KO mouse (Fig. 5A,B). These analyses indicate that transcriptional signatures identified in cultured mouse neurons are also detected in related animal models.

We next examined whether transcriptional signatures are found in disorders that include ASD features but that are not directly caused by loss of one of the five chromatin modifiers we exam-

bivalent modifications at the promoter and modifications that support strong proximal enhancer function, whereas up-regulated genes have modifications that confer strong promoter activity.

Identification of transcriptional signatures in mouse models of syndromic ASD

Although the neuronal cell culture model used here to define transcriptional signatures provides a highly controlled system, its relevance to ASD may not translate to the physiological context of the brain. Therefore, to determine if the transcriptional signatures defined through a primary neuronal culture model are indicative of

ined here. We focused on Fragile X syndrome (FXS), a leading genetic cause of both ID and ASD. FXS is typically caused by a repeat expansion that results in loss of expression of the *FMR1* gene (also known as *FMRP*). FMR1 protein has multiple functions including regulating translation of target mRNAs that encode synaptic proteins (Darnell et al. 2011; Niere et al. 2012) and chromatin modifiers (Korb et al. 2017). We used an *Fmr1* KO mouse model of FXS that recapitulates many aspects of the human disorder (Korb et al. 2017; Spencer et al. 2005, 2008). We found that both by direct overlap and by GSEA analysis (Fig. 5C,D), down-regulated transcriptional signature genes were significantly enriched in genes down-regulated in FXS mouse cortices.
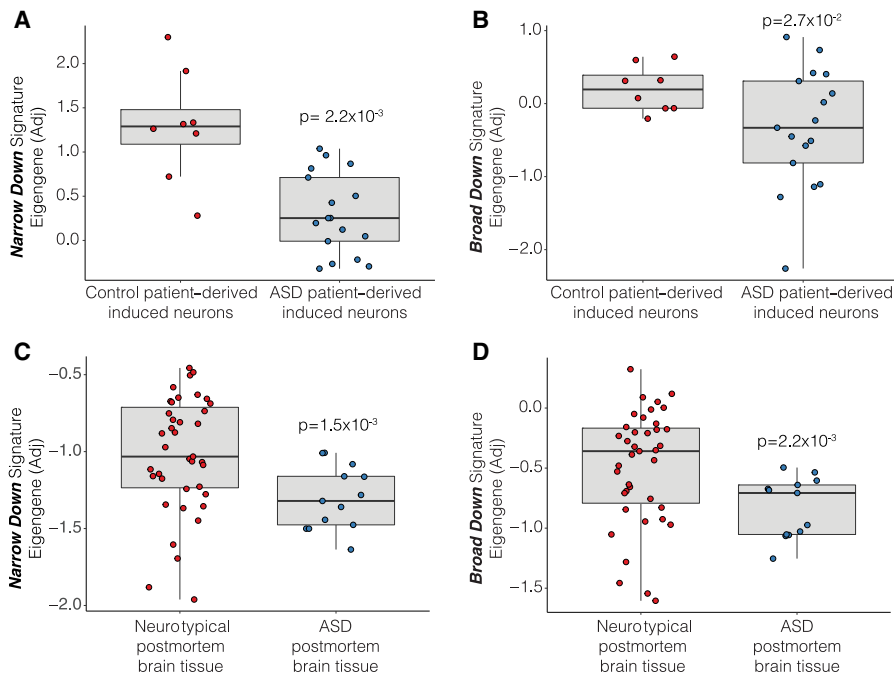
Figure 6. Identification of transcriptional signature in human iPSC-derived neurons with idiopathic ASD. (*A,B*) The eigengene of narrow (*A*) and broad (*B*) down-regulated gene signatures significantly separated idiopathic ASD patient iPSC-derived neurons from controls in work of Marchetto et al. (2017). Linear regression for ASD: (*A*) $P = 2.2 \times 10^{-3}$, (*B*) $P = 2.7 \times 10^{-2}$. (*C,D*) Using data collected from postmortem brain tissue, the eigengene of narrow (*A*) and broad (*B*) down-regulated gene signatures significantly differentiated individuals diagnosed with ASD. Linear regression for ASD: (*C*) $P = 1.5 \times 10^{-3}$, (*D*) $P = 2.2 \times 10^{-3}$. Control indicates neurons derived from neurotypical human iPSCs. (Adj) Adjusted.

Laarhoven et al. 2015). We examined RNA-seq data from a *Kmt2d* KO mouse model (Dhar et al. 2018) and found no significant overlaps or enrichments by GSEA for both broad and narrow signatures (Fig. 5G,H). We also examined a *Kdm6a* KO mouse model and found similarly nonsignificant overlaps, with the exception of a modest overlap between the narrow signature and *Kdm6a* down-regulated genes, and no significant enrichments by GSEA (Supplemental Fig. 7E,F).

To determine whether the lack of enrichment of the transcriptional signature in Kabuki syndrome models was specific to this syndrome, we also examined a mouse model of Williams syndrome. Williams syndrome is an NDD caused by deletion of a region on Chromosome 7 that encompasses 26–28 genes. Williams syndrome results in ID, but rather than causing ASD, patients have a hypersociability phenotype caused by deletion of transcription factors *Gtf2i* and *Gtf2ird1*. Loss of these genes leads to both ID and hypersociability in animal models (Young et al. 2008; Dai et al. 2009; Segura-Puimedon et al. 2014; Barak et al. 2019; Kopp et al. 2019). Using RNA-seq data from hippocampus of a *Gtf2i/Gtf2ird1* double KO mouse model (Kopp et al. 2019), we

found no overlapping gene expression changes with the down-regulated transcriptional signatures (Supplemental Fig. 8A,B). As another control to ensure that any lack of overlap was not just owing to the specific animal model of Williams syndrome chosen, we repeated this analysis with the complete Williams syndrome chromosomal deletion (Kopp et al. 2019). We again found no significant overlap with any differentially expressed genes and found no enrichment through GSEA (Supplemental Fig. 8C,D). These observations demonstrate that the transcriptional signatures defined here are also disrupted in multiple mouse models of ASD but are not observed more broadly in models of other NDDs that only result in ID.

Finally, to interrogate the specificity of these signatures to developmental disorders and as an additional negative control, we repeated these analyses with several models of a neurodegenerative disorder. We examined RNA-seq data from multiple mouse models of Huntington's disease, which is caused by an expansion of the polyglutamine track in the huntingtin (HTT) protein (Langfelder et al. 2016; Yildirim et al. 2019). We used multiple mouse models of Huntington's disease and in most cases either found nonsignificant overlaps and GSEA enrichments or, in some cases, detected inverted enrichments in which the narrow down-regulated gene signature overlapped was enriched in genes up-regulated in the mouse model by GSEA and the narrow up-regulated signature was enriched in genes down-regulated in the mouse model (Supplemental Fig. 9). Next, we repeated all other mouse model comparisons with the up-regulated ASD gene signatures. We found no significant overlap in any of the mouse models used here and only a single significant enrichment by GSEA

Lastly, we examined mouse models of Rett syndrome, which results in global deficits including loss of speech, movement disruptions, and autistic features. It is typically caused by mutations in the gene encoding MECP2, which binds methylated DNA and recruits protein complexes to regulate gene expression (Good et al. 2021). We examined high-quality RNA-seq data obtained from several mouse models of Rett syndrome (Trostle et al. 2021), including a full KO of *Mecp2*, a common *Mecp2* patient mutation, and a heterozygous deletion of *Mecp2* (Pacheco et al. 2017; Jiang et al. 2021). In all cases, we detected a significant overlap of differentially down-regulated genes with the down-regulated transcriptional signatures (Fig. 5E,F; Supplemental Fig. 7A–D). However, genes down-regulated in the mutant model were less significantly enriched for the down-regulated signatures as the *Mecp2* KO by GSEA (Supplemental Fig. 7A,B). Together, these data demonstrate that down-regulated transcriptional signature genes are disrupted in multiple animal models of ASD, even beyond those directly related to the chromatin modifiers used to define this signature in neuronal cultures.

Given these robust findings, we asked whether the transcriptional signatures are detected in any animal model of an NDD in which transcription is disrupted in neurons or whether these signatures are more closely associated with specific phenotypic outcomes such as ID or ASD. To this end, we examined mouse models of Kabuki syndrome, which results in ID and multisystem deficits, including distinct craniofacial features and growth delays, but is not typically associated with ASD. It is caused by mutations in genes encoding either KMT2D (also known as MLL4), which methylates H3K4, or KDM6A, which demethylates H3K27 (Van

(Supplemental Fig. 10; Supplemental Table 9). These analyses suggest the down-regulated gene set as being a more relevant signature that is detected throughout multiple models of syndromic ASD. In addition, these data indicate that the down-regulated transcriptional signatures are disrupted in mouse models of NDDs that result in ASD, but not those that only result in ID, and are absent or even reversed in neurodegenerative disorders. Conversely, the up-regulated transcriptional signatures detected in neuronal cultures are not found in animal models and thus may be more specific to downstream or compensatory changes that are unique to the cell culture experimental model used.

Identification of the transcriptional signature in human ASD iPSCs and tissue

Given that the down-regulated transcriptional signatures were present in multiple animal models of ASD, we next asked whether these signatures are expressed in the brain at times relevant to the development of ASD. To this end, we examined the change in expression of signature genes during early life in mouse neocortical tissue (Fertuzinhos et al. 2014). Regardless of region, averaged gene expression increased during early postnatal life for both up- and down-regulated and both broad and narrow signature genes (Supplemental Fig. 11A–D). In addition, male tissue showed a more enhanced increase compared with female tissue for the down-regulated signatures, suggesting sex-specific differences in the regulation of signature genes. When narrow signature genes are broken down to those specific to activators (CREBBP, ASH1L, NSD1) and those specific to repressors (CHD8 and EHMT1), this developmental increase appeared largely driven by genes regulated by repressors (Supplemental Fig. 11E,F).

Given that human and mouse developmental trajectories happen on different timescales, we also used gene modules identified from BrainSpan data that are expressed at similar levels throughout the human lifespan (Miller et al. 2014; Ji et al. 2016). We found that the transcriptional signatures were highly enriched in several gene modules, including 7 and 36, which peak before birth, as well as additional modules that continue to increase throughout the lifespan (Supplemental Table 10).

Finally, we examined whether signature genes are also disrupted in human patients with ASD. We examined RNA-seq data from induced pluripotent stem cells (iPSCs) derived from idiopathic ASD or neurotypical patients, differentiated into neurons (Marchetto et al. 2017; DeRosa et al. 2018). Given the inherent variability in iPSCs obtained from unrelated individuals, very few significantly differentially expressed genes were detected in these data sets. We therefore used principle component and linear regression analysis to determine if the transcriptional signatures can distinguish the disease state of control and patient samples (Wright et al. 2017; Phan et al. 2020). We found that both the narrow and broad down-regulated transcriptional signatures were sufficient to separate control and ASD iPSC-derived neurons based on the expression of signature genes (Fig. 6A,B). Next, we examined postmortem patients brain tissue from idiopathic ASD or neurotypical patients (Wright et al. 2017). We again found that both the narrow and broad down-regulated transcriptional signatures were sufficient to distinguish between conditions (Fig. 6C,D). Fitting with findings from animal models of ASD, the up-regulated transcriptional signatures were not able to distinguish between control and ASD human iPSC-derived neurons or postmortem tissue (Supplemental Fig. 12A,B). To confirm these findings were not specific to the data set used, we repeated this analysis with additional available data sets using iPSC-derived neurons from control or ASD patients (DeRosa et al. 2018) or postmortem tissue (Parikshak et al. 2016; Velmeshev et al. 2019, 2020). In some cases, we observed similar separations, although the significance of the results and separation of signature eigengenes appeared highly dependent on the sample size of the data set, with nonsignificant results found in lower-powered analyses (Supplemental Fig. 12C–F). Together, these data indicate that the down-regulated transcriptional signatures, defined within primary cultured neurons, were detected within human iPSC-derived neurons from idiopathic ASD patients.

Given the relevance of the down-regulated transcriptional signature gene sets to both mouse and human models of ASD, we sought to determine whether this was a particular asset of the overlap approach we used by placing these analyses in the context of other cross-model comparisons. We therefore examined the extent to which sets of differentially expressed genes identified in primary cell cultures in response to knockdown of single targets were observed in relevant mouse models and human iPSCs derived from patients with mutations in those specific targets (Platt et al. 2017; Deneault et al. 2018; Iacono et al. 2018; Calzari et al. 2020; Lipinski et al. 2020; Fear et al. 2022). We found modest but variable overlap through both direct comparisons of DEGs and linear regression analysis for down-regulated (Supplemental Fig. 13) and up-regulated (Supplemental Fig. 14) genes. In most cases, these direct comparisons were less robust than those made using the transcriptional signature genes. This suggests that the gene set identified through the overlap of targets was more likely to be observed in both mouse tissue and human cell and tissue models of ASD than single-gene sets. In summary, the approaches used here define transcriptional signatures that encode critical neuronal developmental proteins, contain unique chromatin features, and are present throughout multiple experimental models of ASD.

Discussion

Here we defined transcriptional signatures that are shared in response to knockdown of five chromatin-associated proteins linked to NDDs. Characterization of the function of these signatures demonstrated that these genes encoded proteins critical to neuronal development and function, with a notable enrichment in neurotransmitter transport genes and activity-dependent genes. In addition, the chromatin features associated with these signatures were enriched for specific histone modifications such as those encoding bivalent domains. Notably, both the broad and narrow down-regulated transcriptional signatures were significantly enriched in several mouse models of ASD but not in mouse models of NDDs that result in ID in the absence of ASD. Finally, these signatures are sufficient to distinguish between control and idiopathic ASD patient cases.

A major finding that emerged from the analyses described here is that both the broad and narrow down-regulated transcriptional signatures appear to be relevant to a wider range of models of ASD than the up-regulated signatures. We found that the down-regulated signature genes map onto mouse models of NDDs, and both the narrow and broad down-regulated signature genes were able to distinguish between control and ASD patient cells and tissue. Moreover, the human iPSCs and tissue samples were obtained from patients with idiopathic ASD, rather than a disorder resulting from loss of one of the five chromatin modifiers analyzed here. This indicates that this down-regulated transcriptional signature

is relevant to ASD more broadly than the subset of ASD-related syndromes with defined genetic causes.

Although the neuronal culture model used here allows for a highly controlled comparison of the effects of depletion of multiple chromatin modifiers in parallel, it also has several limitations. By its nature, it does not allow for the examination of whether these chromatin modifiers have distinct roles at different time points. It also does not consider very early developmental defects that may result from mutations in chromatin modifiers before cells differentiate into neurons. Further, this system focuses only on neurons in isolation and thus does not capture the more complex results of chromatin disruptions in multiple cell types in the brain and throughout the body. However, these limitations are also what allows for the direct and precise comparison of the immediate transcriptional effects of these chromatin modifiers without the confounding factors of system-wide disruptions and lifelong developmental deficits. This is supported by the finding that transcriptional signatures identified in this system can be identified within the brain of multiple mouse models of related NDDs. This finding suggests that despite limitations, the data described here still provide valuable insights into the link between chromatin misregulation, transcriptional disruptions, and ASD.

The features that cause the disruption of the transcriptional signature genes are not yet clear. It is possible that all five chromatin proteins result in reduced synapse formation or basal firing rate in neurons. This could then lead to transcription changes that are common between all five targets and contribute to the signatures we detected here. However, the enrichment of specific chromatin states in these genes indicates that histone modifications may contribute to their sensitivity to the loss of chromatin-modifying proteins. Similarly, past research has uncovered unusual chromatin features that are found both in the genes whose loss leads to ASD and in genes whose expression is disrupted in idiopathic ASD (Zhao et al. 2018). In our analysis, we found several chromatin features of interest such as the presence of bivalent histone modifications. Because many of the enzymes that control these modifications can be targeted by small-molecule inhibitors, this finding raises the possibility of potentially targeting such modifications to reverse gene expression changes that ultimately lead to ASD. In summary, our data suggest the presence of a transcriptional signature found in multiple models of ASD, suggesting that common transcriptional disruptions may underlie the neuronal dysfunction that ultimately results in ASD and related NDDs.

Methods

Animals

All mice used were on the C57BL/6J background, housed in a 12-h light–dark cycle, and fed a standard diet. All experiments were conducted in accordance with and approval of the IUCAC.

Primary neuronal culture

Cortices were dissected from E16.5 C57BL/6J embryos and cultured in supplemented neurobasal medium (Neurobasal [Gibco 21103-049], B27 [Gibco 17504044], GlutaMAX [Gibco 35050-061], Pen-Strep [Gibco 15140-122]) in TC-treated six-well plates coated with 0.05 mg/mL Poly-D-lysine (Sigma-Aldrich A-003-E). At 3 DIV, neurons were treated with 0.5 μM AraC.

shRNA knockdown

At 5 DIV, neurons were transduced overnight with lentivirus containing an shRNA sequence. Virus was removed the following day (6 DIV), and neurons were cultured for four additional days. shRNA sequences shown in Supplemental Table 12.

Lentivirus production

HEK293T cells were cultured in high-glucose DMEM growth medium (Corning 10-013-CV), 10% FBS (Sigma-Aldrich F2442-500ML), and 1% Pen-Strep (Gibco 15140-122). Calcium phosphate transfection was performed with Pax2 and VSVG packaging plasmids. shRNAs in a pLKO.1-puro backbone were purchased from the Sigma-Aldrich Mission shRNA library (SHCLNG). Viral media was removed 12 h after transfection and collected at 24 and 48 h later. Viral media was passed through a 0.45-μm filter and precipitated overnight with PEG-it solution (40% PEG-8000 [Sigma-Aldrich P2139-1KG], 1.2 M NaCl [Fisher Chemical S271-1]). Viral particles were pelleted and resuspended in 200 μL PBS.

RNA isolation

Total RNA was collected from each transduction at 11 DIV for both RT-qPCR and RNA-seq. RNA for RT-qPCR was isolated from neurons using a Qiagen RNeasy mini kit (74004) or a Zymo Quick-RNA miniprep kit (R1054).

Western blotting

After 10 DIV, neurons were lysed in RIPA (25 mM Tris at pH 7.6, 150 mM NaCl, 1% NP-40, 1% sodium deoxycholate, 0.1% SDS). Protein was resolved by 4%–20% Tris-glycine or 3%–8% Tris-acetate SDS-PAGE, followed by transfer to a 0.45-μm PVDF membrane (Sigma-Aldrich IPVH00010) for immunoblotting. For details, see Supplemental Methods. Antibodies are shown in Supplemental Table 13.

RT-qPCR

cDNA was prepared with a high-capacity cDNA reverse transcription kit (Applied Biosystems 4368813), and quantitative PCR was performed with Power SYBR Green PCR master mix (Applied Biosystems 4367659). Data was analyzed using the common base method (Ganger et al. 2017). Reported statistics were calculated by Student's t-test (two-tailed, heteroscedastic) based on primer efficiency-weighted deltaCT values (ACLM- vs. luciferase-infected). Reported bar graph values represent the square root of the relative expression ratio for a given gene of interest. Primers are shown in Supplemental Table 14.

Immunocytochemistry

For protocol and imaging details, see Supplemental Methods. Antibodies are included in Supplemental Table 13. Cells were imaged on an upright Leica DM 6000, TCS SP8 laser scanning confocal microscope with a 40× HC PL APO CS2 oil objective. Quantification was performed blinded by first counting positively stained cells in each channel. The proportion of excitatory neurons was calculated to be one minus the fraction of total cells that were positive for the GABAergic marker, GAD1.

RNA sequencing

Libraries were generated using the Illumina TruSeq stranded mRNA library prep kit (Illumina 20040534). Libraries were sequenced on an Illumina NextSeq 500/550; reads (75-bp single-end) were mapped to *Mus Musculus* genome build mm10 with

salmon; and the R packages DESeq2 (v3.14) (Love et al. 2014) and *limma* (v3.52.1) via edgeR (v3.38.1) (Robinson et al. 2010) were used to perform differential gene expression analysis. We defined genes as significant using an FDR cutoff of 0.05 and removed genes without an official gene symbol. IGV tools (2.11.3) (Robinson et al. 2011) was used to generate genome browser views.

Statistical analyses

The up- and down-regulated narrow transcriptional signatures were defined separately, using Python 3.9, as the genes that appeared in greater than three of five significantly differentially expressed gene lists. The up- and down-regulated broad transcriptional signatures were defined as genes that were significantly differentially expressed based on a pooled sample model in *limma* (produced by the makeContrasts function as Ash1l + Chd8 + Crebbp + Ehmt1 + Nsd1 vs. luciferase). Genes that were significantly up- or down-regulated in the DESeq2 comparison of no infection versus luciferase shRNA were removed from the directionally appropriate narrow and broad transcriptional signature. Genes removed from each transcriptional signature can be found in Supplemental Table 2. Additional analyses were performed in R (R Core Team 2022). For details of additional analyses performed, see Supplemental Methods.

Data access

All raw and processed sequencing data generated in this study have been submitted to the NCBI Gene Expression Omnibus (GEO; https://www.ncbi.nlm.nih.gov/geo/) under accession number GSE193663. All external data sets used in this study can be found in Supplemental Table 11.

Competing interest statement

The authors declare no competing interests.

Acknowledgments

References

Abrahams BS, Arking DE, Campbell DB, Mefford HC, Morrow EM, Weiss LA, Menashe I, Wadkins T, Banerjee-Basu S, Packer A. 2013. SFARI gene 2.0: a community-driven knowledgebase for the autism spectrum disorders (ASDs). *Mol Autism* **4:** 36. doi:10.1186/2040-2392-4-36

Albert M, Kalebic N, Florio M, Lakshmanaperumal N, Haffner C, Brandl H, Henry I, Huttner WB. 2017. Epigenome profiling and editing of neocortical progenitor cells during development. *EMBO J* **36:** 2642–2658. doi:10.15252/embj.201796764

Barak B, Zhang Z, Liu Y, Nir A, Trangle SS, Ennis M, Levandowski KM, Wang D, Quast K, Boulting GL, et al. 2019. Neuronal deletion of *Gtf2i*, associated with Williams syndrome, causes behavioral and myelin alterations rescuable by a remyelinating drug. *Nat Neurosci* **22:** 700–708. doi:10.1038/s41593-019-0380-9

Bartsch O, Wagner A, Hinkel GK, Krebs P, Stumm M, Schmalenberger B, Böhm S, Balci S, Majewski F. 1999. FISH studies in 45 patients with Rubinstein–Taybi syndrome: deletions associated with polysplenia, hypoplastic left heart and death in infancy. *Eur J Hum Genet* **7:** 748–756. doi:10.1038/sj.ejhg.5200378

Benevento M, Iacono G, Selten M, Ba W, Oudakker A, Frega M, Keller J, Mancini R, Lewerissa E, Kleefstra T, et al. 2016. Histone methylation by the Kleefstra syndrome protein EHMT1 mediates homeostatic synaptic scaling. *Neuron* **91:** 341–355. doi:10.1016/j.neuron.2016.06.003

Berger SL. 2007. The complex language of chromatin regulation during transcription. *Nature* **447:** 407–412. doi:10.1038/nature05915

Bernier R, Golzio C, Xiong B, Stessman HA, Coe BP, Penn O, Witherspoon K, Gerdts J, Baker C, Vulto-Van Silfhout AT, et al. 2014. Disruptive *CHD8* mutations define a subtype of autism early in development. *Cell* **158:** 263–276. doi:10.1016/j.cell.2014.06.017

Bernstein BE, Mikkelsen TS, Xie X, Kamal M, Huebert DJ, Cuff J, Fry B, Meissner A, Wernig M, Plath K, et al. 2006. A bivalent chromatin structure marks key developmental genes in embryonic stem cells. *Cell* **125:** 315–326. doi:10.1016/j.cell.2006.02.041

Borrelli E, Nestler EJ, Allis CD, Sassone-Corsi P. 2008. Decoding the epigenetic language of neuronal plasticity. *Neuron* **60:** 961–974. doi:10.1016/j.neuron.2008.10.012

Brockes JP, Fields KL, Raff MC. 1979. Studies on cultured rat Schwann cells. I. Establishment of purified populations from cultures of peripheral nerve. *Brain Res* **165:** 105–118. doi:10.1016/0006-8993(79)90048-9

Calzari L, Barcella M, Alari V, Braga D, Muñoz-Viana R, Barlassina C, Finelli P, Gervasini C, Barco A, Russo S, et al. 2020. Transcriptome analysis of iPSC-derived neurons from Rubinstein–Taybi patients reveals deficits in neuronal differentiation. *Mol Neurobiol* **57:** 3685–3701. doi:10.1007/s12035-020-01983-6

Chen MB, Jiang X, Quake SR, Südhof TC. 2020. Persistent transcriptional programmes are associated with remote memory. *Nature* **587:** 437–442. doi:10.1038/s41586-020-2905-5

Coupry I, Roudaut C, Stef M, Delrue M-A, Marche M, Burgelin I, Taine L, Cruaud C, Lacombe D, Arveiler B. 2002. Molecular analysis of the *CBP* gene in 60 patients with Rubinstein–Taybi syndrome. *J Med Genet* **39:** 415–421. doi:10.1136/jmg.39.6.415

Dai L, Bellugi U, Chen X-N, Pulst-Korenberg AM, Järvinen-Pasley A, Tirosh-Wagner T, Eis PS, Graham J, Mills D, Searcy Y, et al. 2009. Is it Williams syndrome? *GTF2IRD1* implicated in visual-spatial construction and *GTF2I* in sociability revealed by high resolution arrays. *Am J Med Genet A* **149A:** 302–314. doi:10.1002/ajmg.a.32652

Darnell JC, Van Driesche SJ, Zhang C, Hung KYS, Mele A, Fraser CE, Stone EF, Chen C, Fak JJ, Chi SW, et al. 2011. FMRP stalls ribosomal translocation on mRNAs linked to synaptic function and autism. *Cell* **146:** 247–261. doi:10.1016/j.cell.2011.06.013

Deneault E, White SH, Rodrigues DC, Ross PJ, Faheem M, Zaslavsky K, Wang Z, Alexandrova R, Pellecchia G, Wei W, et al. 2018. Complete disruption of autism-susceptibility genes by gene editing predominantly reduces functional connectivity of isogenic human neurons. *Stem Cell Rep* **11:** 1211–1225. doi:10.1016/j.stemcr.2018.10.003

DeRosa BA, El Hokayem J, Artimovich E, Garcia-Serje C, Phillips AW, Van Booven D, Nestor JE, Wang L, Cuccaro ML, Vance JM, et al. 2018. Convergent pathways in idiopathic autism revealed by time course transcriptomic analysis of patient-derived neurons. *Sci Rep* **8:** 8423. doi:10.1038/s41598-018-26495-1

De Rubeis S, He X, Goldberg AP, Poultney CS, Samocha K, Cicek AE, Kou Y, Liu L, Fromer M, Walker S, et al. 2014. Synaptic, transcriptional and chromatin genes disrupted in autism. *Nature* **515:** 209–215. doi:10.1038/nature13772

Dhar SS, Zhao D, Lin T, Gu B, Pal K, Wu SJ, Alam H, Lv J, Yun K, Gopalakrishnan V, et al. 2018. MLL4 is required to maintain broad H3K4me3 peaks and super-enhancers at tumor suppressor genes. *Mol Cell* **70:** 825–841.e6. doi:10.1016/j.molcel.2018.04.028

Dotti C, Sullivan C, Banker G. 1988. The establishment of polarity by hippocampal neurons in culture. *J Neurosci* **8:** 1454–1468. doi:10.1523/JNEUROSCI.08-04-01454.1988

Douglas J, Hanks S, Temple IK, Davies S, Murray A, Upadhyaya M, Tomkins S, Hughes HE, Trevor Cole RP, Rahman N. 2003. *NSD1* mutations are the major cause of Sotos syndrome and occur in some cases of weaver syndrome but are rare in other overgrowth phenotypes. *Am J Hum Genet* **72:** 132–143. doi:10.1086/345647

Eram MS, Kuznetsova E, Li F, Lima-Fernandes E, Kennedy S, Chau I, Arrowsmith CH, Schapira M, Vedadi M. 2015. Kinetic characterization of human histone H3 lysine 36 methyltransferases, ASH1L and SETD2. *Biochim Biophys Acta* **1850:** 1842–1848. doi:10.1016/j.bbagen.2015.05.013

Ernst J, Kellis M. 2017. Chromatin-state discovery and genome annotation with ChromHMM. *Nat Protoc* **12:** 2478–2492. doi:10.1038/nprot.2017.124

Fear VS, Forbes CA, Anderson D, Rauschert S, Syn G, Shaw N, Jamieson S, Ward M, Baynam G, Lassmann T. 2022. CRISPR single base editing, neuronal disease modelling and functional genomics for genetic variant analysis: pipeline validation using Kleefstra syndrome EHMT1 haploinsufficiency. *Stem Cell Res Ther* **13:** 69. doi:10.1186/s13287-022-02740-3

Fertuzinhos S, Li M, Kawasawa YI, Ivic V, Franjic D, Singh D, Crair M, Šestan N. 2014. Laminar and temporal expression dynamics of coding and

noncoding RNAs in the mouse neocortex. *Cell Rep* **6:** 938–950. doi:10.1016/j.celrep.2014.01.036

Frank CL, Tsai L-H. 2009. Alternative functions of core cell cycle regulators in neuronal migration, neuronal maturation, and synaptic plasticity. *Neuron* **62:** 312–326. doi:10.1016/j.neuron.2009.03.029

Fu JM, Satterstrom FK, Peng M, Brand H, Collins RL, Dong S, Klei L, Stevens CR, Cusick C, Babadi M, et al. 2021. Rare coding variation illuminates the allelic architecture, risk genes, cellular expression patterns, and phenotypic context of autism. medRxiv doi:10.1101/2021.12.20.21267194

Ganger MT, Dietz GD, Ewing SJ. 2017. A common base method for analysis of qPCR data and the application of simple blocking in qPCR experiments. *BMC Bioinformatics* **18:** 534. doi:10.1186/s12859-017-1949-5

Gao Y, Duque-Wilckens N, Aljazi MB, Wu Y, Moeser AJ, Mias GI, Robison AJ, He J. 2021. Loss of histone methyltransferase ASH1L in the developing mouse brain causes autistic-like behaviors. *Commun Biol* **4:** 756. doi:10.1038/s42003-021-02282-z

Good KV, Vincent JB, Ausió J. 2021. MeCP2: the genetic driver of Rett syndrome epigenetics. *Front Genet* **12:** 620859. doi:10.3389/fgene.2021.620859

Huang E, Qu D, Zhang Y, Venderova K, Haque ME, Rousseaux MWC, Slack RS, Woulfe JM, Park DS. 2010. The role of Cdk5-mediated apurinic/apyrimidinic endonuclease 1 phosphorylation in neuronal death. *Nat Cell Biol* **12:** 563–571. doi:10.1038/ncb2058

Iacono G, Dubos A, Méziane H, Benevento M, Habibi E, Mandoli A, Riet F, Selloum M, Feil R, Zhou H, et al. 2018. Increased H3K9 methylation and impaired expression of protocadherins are associated with the cognitive dysfunctions of the Kleefstra syndrome. *Nucleic Acids Res* **46:** 4950–4965. doi:10.1093/nar/gky196

Ietswaart R, Gyori BM, Bachman JA, Sorger PK, Churchman LS. 2021. GeneWalk identifies relevant gene functions for a biological context using network representation learning. *Genome Biol* **22:** 55. doi:10.1186/s13059-021-02264-8

Iossifov I, O'Roak BJ, Sanders SJ, Ronemus M, Krumm N, Levy D, Stessman HA, Witherspoon KT, Vives L, Patterson KE, et al. 2014. The contribution of de novo coding mutations to autism spectrum disorder. *Nature* **515:** 216–221. doi:10.1038/nature13908

Jenuwein T, Allis CD. 2001. Translating the histone code. *Science* **293:** 1074–1080. doi:10.1126/science.1063127

Ji X, Kember RL, Brown CD, Bućan M. 2016. Increased burden of deleterious variants in essential genes in autism spectrum disorder. *Proc Natl Acad Sci* **113:** 15054–15059. doi:10.1073/pnas.1613195113

Jiang Y, Fu X, Zhang Y, Wang S-F, Zhu H, Wang W-K, Zhang L, Wu P, Wong CCL, Li J, et al. 2021. Rett syndrome linked to defects in forming the MeCP2/Rbfox/LASR complex in mouse models. *Nat Commun* **12:** 5767. doi:10.1038/s41467-021-26084-3

Jin Q, Yu L-R, Wang L, Zhang Z, Kasper LH, Lee J-E, Wang C, Brindle PK, Dent SYR, Ge K. 2011. Distinct roles of GCN5/PCAF-mediated H3K9ac and CBP/p300-mediated H3K18/27ac in nuclear receptor transactivation: histone acetylation and gene activation. *EMBO J* **30:** 249–262. doi:10.1038/emboj.2010.318

Kleefstra T, Brunner HG, Amiel J, Oudakker AR, Nillesen WM, Magee A, Geneviève D, Cormier-Daire V, van Esch H, Fryns J-P, et al. 2006. Loss-of-function mutations in *euchromatin histone methyl transferase 1 (EHMT1)* cause the 9q34 subtelomeric deletion syndrome. *Am J Hum Genet* **79:** 370–377. doi:10.1086/505693

Kleefstra T, van Zelst-Stams WA, Nillesen WM, Cormier-Daire V, Houge G, Foulds N, van Dooren M, Willemsen MH, Pfundt R, Turner A, et al. 2009. Further clinical and molecular delineation of the 9q subtelomeric deletion syndrome supports a major contribution of *EHMT1* haploinsufficiency to the core phenotype. *J Med Genet* **46:** 598–606. doi:10.1136/jmg.2008.062950

Kopp N, McCullough K, Maloney SE, Dougherty JD. 2019. *Gtf2i* and *Gtf2ird1* mutation do not account for the full phenotypic effect of the Williams syndrome critical region in mouse models. *Hum Mol Genet* **28:** 3443–3465. doi:10.1093/hmg/ddz176

Korb E, Herre M, Zucker-Scharff I, Darnell RB, Allis CD. 2015. BET protein Brd4 activates transcription in neurons and BET inhibitor Jq1 blocks memory in mice. *Nat Neurosci* **18:** 1464–1473. doi:10.1038/nn.4095

Korb E, Herre M, Zucker-Scharff I, Gresack J, Allis CD, Darnell RB. 2017. Excess translation of epigenetic regulators contributes to fragile X syndrome and is alleviated by Brd4 inhibition. *Cell* **170:** 1209–1223.e20. doi:10.1016/j.cell.2017.07.033

Kurotaki N, Imaizumi K, Harada N, Masuno M, Kondoh T, Nagai T, Ohashi H, Naritomi K, Tsukahara M, Makita Y, et al. 2002. Haploinsufficiency of *NSD1* causes Sotos syndrome. *Nat Genet* **30:** 365–366. doi:10.1038/ng863

Langfelder P, Cantle JP, Chatzopoulou D, Wang N, Gao F, Al-Ramahi I, Lu X-H, Ramos EM, El-Zein K, Zhao Y, et al. 2016. Integrated genomics and proteomics define Huntingtin CAG length-dependent networks in mice. *Nat Neurosci* **19:** 623–633. doi:10.1038/nn.4256

Law CW, Chen Y, Shi W, Smyth GK. 2014. Voom: precision weights unlock linear model analysis tools for RNA-seq read counts. *Genome Biol* **15:** R29. doi:10.1186/gb-2014-15-2-r29

Lim S, Kaldis P. 2013. Cdks, cyclins and CKIs: roles beyond cell cycle regulation. *Development* **140:** 3079–3093. doi:10.1242/dev.091744

Lipinski M, Muñoz-Viana R, del Blanco B, Marquez-Galera A, Medrano-Relinque J, Caramés JM, Szczepankiewicz AA, Fernandez-Albert J, Navarrón CM, Olivares R, et al. 2020. KAT3-dependent acetylation of cell type-specific genes maintains neuronal identity in the adult mouse brain. *Nat Commun* **11:** 2588. doi:10.1038/s41467-020-16246-0

Love MI, Huber W, Anders S. 2014. Moderated estimation of fold change and dispersion for RNA-seq data with DESeq2. *Genome Biol* **15:** 550. doi:10.1186/s13059-014-0550-8

Marchetto MC, Belinson H, Tian Y, Freitas BC, Fu C, Vadodaria KC, Beltrao-Braga PC, Trujillo CA, Mendes APD, Padmanabhan K, et al. 2017. Altered proliferation and networks in neural cells derived from idiopathic autistic individuals. *Mol Psychiatry* **22:** 820–835. doi:10.1038/mp.2016.95

Mi H, Ebert D, Muruganujan A, Mills C, Albou L-P, Mushayamaha T, Thomas PD. 2021. PANTHER version 16: a revised family classification, tree-based classification tool, enhancer regions and extensive API. *Nucleic Acids Res* **49:** D394–D403. doi:10.1093/nar/gkaa1106

Miller JA, Ding S-L, Sunkin SM, Smith KA, Ng L, Szafer A, Ebbert A, Riley ZL, Royall JJ, Aiona K, et al. 2014. Transcriptional landscape of the prenatal human brain. *Nature* **508:** 199–206. doi:10.1038/nature13185

Miyazaki H, Higashimoto K, Yada Y, Endo TA, Sharif J, Komori T, Matsuda M, Koseki Y, Nakayama M, Soejima H, et al. 2013. Ash1l methylates Lys36 of histone H3 independently of transcriptional elongation to counteract polycomb silencing. *PLoS Genet* **9:** e1003897. doi:10.1371/journal.pgen.1003897

Neale BM, Kou Y, Liu L, Ma'ayan A, Samocha KE, Sabo A, Lin C-F, Stevens C, Wang L-S, Makarov V, et al. 2012. Patterns and rates of exonic de novo mutations in autism spectrum disorders. *Nature* **485:** 242–245. doi:10.1038/nature11011

Niere F, Wilkerson JR, Huber KM. 2012. Evidence for a fragile X mental retardation protein-mediated translational switch in metabotropic glutamate receptor-triggered Arc translation and long-term depression. *J Neurosci* **32:** 5924–5936. doi:10.1523/JNEUROSCI.4650-11.2012

Niikawa N. 2004. Molecular basis of Sotos syndrome. *Horm Res* **62**(Suppl 3): 60–65. doi:10.1159/000080501

Ohnuma S, Harris WA. 2003. Neurogenesis and the cell cycle. *Neuron* **40:** 199–208. doi:10.1016/S0896-6273(03)00632-9

Okamoto N, Miya F, Tsunoda T, Kato M, Saitoh S, Yamasaki M, Kanemura Y, Kosaki K. 2017. Novel MCA/ID syndrome with *ASH1L* mutation. *Am J Med Genet A* **173:** 1644–1648. doi:10.1002/ajmg.a.38193

O'Roak BJ, Vives L, Girirajan S, Karakoc E, Krumm N, Coe BP, Levy R, Ko A, Lee C, Smith JD, et al. 2012. Sporadic autism exomes reveal a highly interconnected protein network of de novo mutations. *Nature* **485:** 246–250. doi:10.1038/nature10989

Pacheco NL, Heaven MR, Holt LM, Crossman DK, Boggio KJ, Shaffer SA, Flint DL, Olsen ML. 2017. RNA sequencing and proteomics approaches reveal novel deficits in the cortex of *Mecp2*-deficient mice, a model for Rett syndrome. *Mol Autism* **8:** 56. doi:10.1186/s13229-017-0174-4

Parikshak NN, Luo R, Zhang A, Won H, Lowe JK, Chandran V, Horvath S, Geschwind DH. 2013. Integrative functional genomic analyses implicate specific molecular pathways and circuits in autism. *Cell* **155:** 1008–1021. doi:10.1016/j.cell.2013.10.031

Parikshak NN, Swarup V, Belgard TG, Irimia M, Ramaswami G, Gandal MJ, Hartl C, Leppa V, de la Torre Ubieta L, Huang J, et al. 2016. Genome-wide changes in lncRNA, splicing, and regional gene expression patterns in autism. *Nature* **540:** 423–427. doi:10.1038/nature20612

Peixoto L, Abel T. 2013. The role of histone acetylation in memory formation and cognitive impairments. *Neuropsychopharmacology* **38:** 62–76. doi:10.1038/npp.2012.86

Petrif F, Giles RH, Dauwerse HG, Saris JJ, Hennekam RCM, Masuno M, Tommerup N, van Ommen G-JB, Goodman RH, Peters DJM, et al. 1995. Rubinstein–Taybi syndrome caused by mutations in the transcriptional co-activator CBP. *Nature* **376:** 348–351. doi:10.1038/376348a0

Phan BN, Bohlen JF, Davis BA, Ye Z, Chen H-Y, Mayfield B, Sripathy SR, Cerceo Page S, Campbell MN, Smith HL, et al. 2020. A myelin-related transcriptomic profile is shared by Pitt–Hopkins syndrome models and human autism spectrum disorder. *Nat Neurosci* **23:** 375–385. doi:10.1038/s41593-019-0578-x

Platt RJ, Zhou Y, Slaymaker IM, Shetty AS, Weisbach NR, Kim J-A, Sharma J, Desai M, Sood S, Kempton HR, et al. 2017. *Chd8* mutation leads to autistic-like behaviors and impaired striatal circuits. *Cell Rep* **19:** 335–350. doi:10.1016/j.celrep.2017.03.052

Qiao Q, Li Y, Chen Z, Wang M, Reinberg D, Xu R-M. 2011. The structure of NSD1 reveals an autoregulatory mechanism underlying histone H3K36 methylation. *J Biol Chem* **286:** 8361–8368. doi:10.1074/jbc.M110.204115

Rangasamy S, D'Mello SR, Narayanan V. 2013. Epigenetics, autism spectrum, and neurodevelopmental disorders. *Neurotherapeutics* **10:** 742–756. doi:10.1007/s13311-013-0227-0

R Core Team. 2022. *R: a language and environment for statistical computing*. R Foundation for Statistical Computing, Vienna. https://www.R-project.org/.

Ritchie ME, Phipson B, Wu D, Hu Y, Law CW, Shi W, Smyth GK. 2015. *limma* powers differential expression analyses for RNA-sequencing and microarray studies. *Nucleic Acids Res* **43:** e47. doi:10.1093/nar/gkv007

Robinson MD, McCarthy DJ, Smyth GK. 2010. edgeR: a Bioconductor package for differential expression analysis of digital gene expression data. *Bioinformatics* **26:** 139–140. doi:10.1093/bioinformatics/btp616

Robinson JT, Thorvaldsdóttir H, Winckler W, Guttman M, Lander ES, Getz G, Mesirov JP. 2011. Integrative genomics viewer. *Nat Biotechnol* **29:** 24–26. doi:10.1038/nbt.1754

Sanders SJ, Murtha MT, Gupta AR, Murdoch JD, Raubeson MJ, Willsey AJ, Ercan-Sencicek AG, DiLullo NM, Parikshak NN, Stein JL, et al. 2012. *De novo* mutations revealed by whole-exome sequencing are strongly associated with autism. *Nature* **485:** 237–241. doi:10.1038/nature10945

Schorry EK, Keddache M, Lanphear N, Rubinstein JH, Srodulski S, Fletcher D, Blough-Pfau RI, Grabowski GA. 2008. Genotype–phenotype correlations in Rubinstein–Taybi syndrome. *Am J Med Genet A* **146A:** 2512–2519. doi:10.1002/ajmg.a.32424

Segura-Puimedon M, Sahún I, Velot E, Dubus P, Borralleras C, Rodrigues AJ, Valero MC, Valverde O, Sousa N, Herault Y, et al. 2014. Heterozygous deletion of the Williams–Beuren syndrome critical interval in mice recapitulates most features of the human disorder. *Hum Mol Genet* **23:** 6481–6494. doi:10.1093/hmg/ddu368

Shen W, Krautscheid P, Rutz AM, Bayrak-Toydemir P, Dugan SL. 2019. *De novo* loss-of-function variants of *ASH1L* are associated with an emergent neurodevelopmental disorder. *Eur J Med Genet* **62:** 55–60. doi:10.1016/j.ejmg.2018.05.003

Spencer CM, Alekseyenko O, Serysheva E, Yuva-Paylor LA, Paylor R. 2005. Altered anxiety-related and social behaviors in the *Fmr1* knockout mouse model of fragile X syndrome. *Genes Brain Behav* **4:** 420–430. doi:10.1111/j.1601-183X.2005.00123.x

Spencer CM, Graham DF, Yuva-Paylor LA, Nelson DL, Paylor R. 2008. Social behavior in *Fmr1* knockout mice carrying a human *FMR1* transgene. *Behav Neurosci* **122:** 710–715. doi:10.1037/0735-7044.122.3.710

Stessman HAF, Xiong B, Coe BP, Wang T, Hoekzema K, Fenckova M, Kvarnung M, Gerdts J, Trinh S, Cosemans N, et al. 2017. Targeted sequencing identifies 91 neurodevelopmental-disorder risk genes with autism and developmental-disability biases. *Nat Genet* **49:** 515–526. doi:10.1038/ng.3792

Strahl BD, Allis CD. 2000. The language of covalent histone modifications. *Nature* **403:** 41–45. doi:10.1038/47412

Supek F, Bošnjak M, Škunca N, Šmuc T. 2011. REVIGO summarizes and visualizes long lists of Gene Ontology terms. *PLoS One* **6:** e21800. doi:10.1371/journal.pone.0021800

Tachibana M, Matsumura Y, Fukuda M, Kimura H, Shinkai Y. 2008. G9a/GLP complexes independently mediate H3K9 and DNA methylation to silence transcription. *EMBO J* **27:** 2681–2690. doi:10.1038/emboj.2008.192

Tanaka Y, Naruse I, Maekawa T, Masuya H, Shiroishi T, Ishii S. 1997. Abnormal skeletal patterning in embryos lacking a single *Cbp* allele: a partial similarity with Rubinstein–Taybi syndrome. *Proc Natl Acad Sci* **94:** 10215–10220. doi:10.1073/pnas.94.19.10215

Thompson BA, Tremblay V, Lin G, Bochar DA. 2008. CHD8 is an ATP-dependent chromatin remodeling factor that regulates β-catenin target genes. *Mol Cell Biol* **28:** 3894–3904. doi:10.1128/MCB.00322-08

Trostle AJ, Li L, Kim S-Y, Wang J, Al-Ouran R, Yalamanchili HK, Liu Z, Wan Y-W. 2021. MECP2pedia: a comprehensive transcriptome portal for MECP2 disease research. bioRxiv doi:10.1101/2021.11.27.470197

Turner BM. 2000. Histone acetylation and an epigenetic code. *BioEssays* **22:** 836–845. doi:10.1002/1521-1878(200009)22:9<836::AID-BIES9>3.0.CO;2-X

Van Laarhoven PM, Neitzel LR, Quintana AM, Geiger EA, Zackai EH, Clouthier DE, Artinger KB, Ming JE, Shaikh TH. 2015. Kabuki syndrome genes *KMT2D* and *KDM6A*: functional analyses demonstrate critical roles in craniofacial, heart and brain development. *Hum Mol Genet* **24:** 4443–4453. doi:10.1093/hmg/ddv180

Velmeshev D, Schirmer L, Jung D, Haeussler M, Perez Y, Mayer S, Bhaduri A, Goyal N, Rowitch DH, Kriegstein AR. 2019. Single-cell genomics identifies cell type–specific molecular changes in autism. *Science* **364:** 685–689. doi:10.1126/science.aav8130

Velmeshev D, Magistri M, Mazza EMC, Lally P, Khoury N, D'Elia ER, Bicciato S, Faghihi MA. 2020. Cell-type-specific analysis of molecular pathology in autism identifies common genes and pathways affected across neocortical regions. *Mol Neurobiol* **57:** 2279–2289. doi:10.1007/s12035-020-01879-5

Voigt P, Tee W-W, Reinberg D. 2013. A double take on bivalent promoters. *Genes Dev* **27:** 1318–1338. doi:10.1101/gad.219626.113

Wright C, Shin JH, Rajpurohit A, Deep-Soboslay A, Collado-Torres L, Brandon NJ, Hyde TM, Kleinman JE, Jaffe AE, Cross AJ, et al. 2017. Altered expression of histamine signaling genes in autism spectrum disorder. *Transl Psychiatry* **7:** e1126. doi:10.1038/tp.2017.87

Yildirim F, Ng CW, Kappes V, Ehrenberger T, Rigby SK, Stivanello V, Gipson TA, Soltis AR, Vanhoutte P, Caboche J, et al. 2019. Early epigenomic and transcriptional changes reveal Elk-1 transcription factor as a therapeutic target in Huntington's disease. *Proc Natl Acad Sci* **116:** 24840–24851. doi:10.1073/pnas.1908113116

Young EJ, Lipina T, Tam E, Mandel A, Clapcote SJ, Bechard AR, Chambers J, Mount HTJ, Fletcher PJ, Roder JC, et al. 2008. Reduced fear and aggression and altered serotonin metabolism in *Gtf2ird1*-targeted mice. *Genes Brain Behav* **7:** 224–234. doi:10.1111/j.1601-183X.2007.00343.x

Zhao Y-T, Kwon DY, Johnson BS, Fasolino M, Lamonica JM, Kim YJ, Zhao BS, He C, Vahedi G, Kim TH, et al. 2018. Long genes linked to autism spectrum disorders harbor broad enhancer-like chromatin domains. *Genome Res* **28:** 933–942. doi:10.1101/gr.233775.117